Electronic and structural properties of GaAs(100)(2×4) and InAs(100)(2×4) surfaces studied by core-level photoemission and scanning tunneling microscopy

P. Laukkanen,* M. Kuzmin,† R. E. Perälä, M. Ahola, S. Mattila, and I. J. Väyrynen
Department of Physics, University of Turku, FIN-20014 Turku, Finland

J. Sadowski
MAX-lab, Lund University, SE-221 00 Lund, Sweden and Institute of Physics, Polish Academy of Sciences, al. Lotnikow 32/46, 02-668 Warszawa, Poland

J. Konttinen, T. Jouhti, C. S. Peng, M. Saarinen, and M. Pessa
Optoelectronics Research Centre, Tampere University of Technology, P.O. Box 692, FIN-33101 Tampere, Finland
(Received 1 February 2005; revised manuscript received 4 April 2005; published 12 July 2005)

Electronic and structural properties of GaAs(100)(2×4), InAs(100)(2×4), and Sb/InAs(100)(2×4) reconstructed surfaces have been studied by synchrotron-radiation photoelectron spectroscopy and scanning tunneling microscopy (STM). Based on the difference spectrum of As 3*d* core-level spectra of III-As(100)(2×4), measured in different surface-sensitivity conditions, as well as the line shape of the As 3*d* emission from the Sb-induced (2×4) surface, we give evidence that the As 3*d* spectra of GaAs(100)(2×4) and InAs(100)(2×4) consist of two surface-core-level-shifted components. One of them is shifted about 0.2 eV to the lower kinetic energy from the bulk component. On the basis of the relative component intensities, this surface-shifted As 3*d* component is assigned to the emission from the first-layer As dimers in the established model of the (2×4) surface. The other component, shifted about 0.3 eV to the higher kinetic energy, is connected to the third-layer As-dimer site. The comparison of the core-level results between GaAs(100)(2×4) and InAs(100)×(2×4) suggests that the $\alpha 2$ phase, which has one As dimer in both the first and third atomic layers per unit cell, exists on GaAs(100)(2×4), similarly to the case of InAs(100)(2×4), as predicted in theory but not observed to date. Furthermore, the STM observation of the GaAs(100)(2×4)$\alpha 2$ phase is reported.

DOI: 10.1103/PhysRevB.72.045321 PACS number(s): 73.20.-r, 68.35.-p, 81.10.-h

I. INTRODUCTION

Single-crystal III-V compound semiconductors with the reconstructed (100)(2×4) surfaces, generated under a wide range of epitaxial growth conditions, are the most common substrates used for preparing heterostructures for electronic and optoelectronic applications by means of molecular-beam epitaxy (MBE).[1,2] Knowledge of the electronic, structural, and chemical properties of this particular surface contributes to the understanding of the initial stages of epitaxy and physical properties of interfaces, which determine device performance features.

The following principles are believed to explain the reconstruction on the III-V(100) surface.[3] (i) Surface atoms dimerize to reduce the number of unsaturated dangling bonds. (ii) Uncharged surfaces have all dangling-bond states filled in the valence band, while the conduction band is empty according to the electron counting model (ECM), predicting missing dimers; i.e., vacant dimer sites. (iii) Spatial arrangement of dimers minimizes the electrostatic energy. The principles (i)–(iii) are obeyed by the so-called $\beta 2$ structural model [Fig. 1(c)], which has been confirmed for the GaAs(100)(2×4) and InAs(100)(2×4) surfaces.[4–16] The $\beta 2$ structure consists of two As dimers in the top (first) atomic layer and one As dimer in the third layer per unit cell, thus giving rise to the surface As coverage of 0.75 ML. At the lower coverage, 0.5 ML, GaAs(100)(2×4) and InAs(100)×(2×4) exhibit an interesting difference; namely, the GaAs(100)(2×4) surface has the α structure,[5,6,17] while the InAs(100)(2×4) surface has the $\alpha 2$ structure.[7,13,16] The α phase is composed of two As dimers in the first atomic layer and two group-III dimers in the second layer per unit cell; the $\alpha 2$ phase has one As dimer in the first and third layers and two group-III dimers in the second layer (Fig. 1). These two phases have the same number of As dimers and As and cation dangling bonds, but the electrostatic energy of the $\alpha 2$ phase is lower than that of the α one;[14] hence, the $\alpha 2$ model agrees with the item (iii). According to the theory,[13–15] the $\alpha 2$ phase should also appear on the GaAs(100)(2×4) surface, but it has never been observed.

Other open issues regarding the III-V(100)(2×4) surfaces are the number and the physical origin of surface-core-

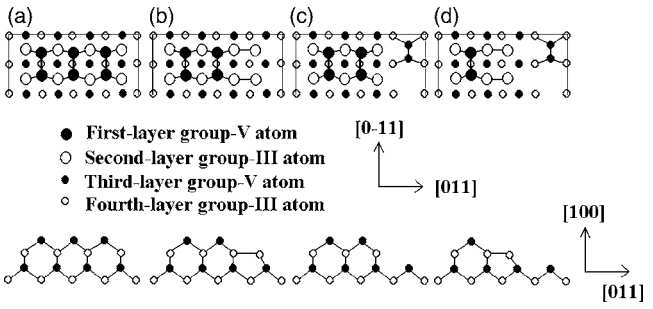

FIG. 1. Some atomic models with the cross sections for the III-V(100)(2×4) reconstruction: (a) β, (b) α, (c) $\beta 2$, and (d) $\alpha 2$.

 ©2005 The American Physical Society

level-shifts (SCLS's) in the photoemission spectra. Such SCLS's are related to the charge transfer and electronic screening on the solid surface,[18,19] and reflect different bonding sites of the atoms in the interface. Even though the core-level photoemission is not a direct structural probe, it carries quantitative information about the atomic bonding sites if the core-level-line shape and fine-structures of the spectra are known accurately, as stressed previously.[20,21]

Earlier studies have shown that the As 3*d* and Ga 3*d* spectra of GaAs(100)(2×4) can be interpreted as due to one or two surface components besides the bulk one.[21–27] Each model in Fig. 1 includes two or more nonequivalent surface or subsurface sites per unit cell, and all of them can contribute to the photoemission. The SCLS's have been previously attributed to As dimers, while Ga-related SCLS's are interpreted as due to the second-layer atoms below the As dimers. Yet, there exists no consensus about the atomic origins of the SCLS's. On the basis of the geometrical and chemical similarities between InAs(100)(2×4) and GaAs(100)(2×4),[12,13,15] the SCLS's for these surfaces should resemble each other. To date, however, no SCLS investigation seems to have been reported on the clean InAs(100)(2×4) surface.

From these perspectives, we have investigated GaAs(100)(2×4) and InAs(100)(2×4) surfaces by core-level photoelectron spectroscopy utilizing synchrotron radiation and by scanning tunneling microscopy (STM). The paper is organized as follows. First we present filled-state STM images of GaAs(100)(2×4), which allow us to identify the $\alpha 2$ structure. Then emphasis has been addressed to the As 3*d* spectra from the Sb-induced InAs(100)(2×4) and clean InAs(100)(2×4) and GaAs(100)(2×4) surfaces. The presented spectra are rather featureless, and the spectral components overlap each other. It is well known that the deconvolution (fitting) of such spectra alone may not prove the number of SCLS's that actually exist. Therefore, to clarify the surface-related spectral features and to justify the presence of SCLS's found, we have analyzed a so-called difference line shape for two spectra measured in different surface-sensitive conditions by varying the emission angle and kinetic energy of photoelectrons. Furthermore, the As 3*d* emission from the Sb/InAs(100)(2×4) surface, where the substitution of surface As-dimer atoms by Sb is shown to occur similarly to the Sb/GaAs(100)(2×4) system,[28–35] provides the As 3*d* line shape for components used in the fittings.

The results verify that the As 3*d* emission from the clean III-As(100)(2×4) surface consists of at least two SCLS's. One of these SCLS's, which is shifted about 0.2 eV to the lower kinetic energy (higher binding energy) from the bulk component, has not been observed earlier, to the best of our knowledge. Moreover, the comparison of the core-level results between the GaAs(100)(2×4) and InAs(100)(2×4), combined with the STM observations, show that the $\alpha 2$ domains appear on the GaAs(100)(2×4) surface in agreement with the InAs(100)(2×4) system.

II. EXPERIMENTS

Photoemission was measured at the Swedish National Synchrotron Radiation Center MAX-lab (beamline 41). An incidence angle of *p*-polarized light was 45° relative to the surface normal. The spectra were taken using a hemispherical electron energy analyzer with an angular resolution better than 2° and a total energy resolution better than 0.25 eV. In order to study the surface sensitivity of the spectral features, the photon energy and electron-emission angle (from the normal) were varied.

STM measurements on GaAs(100)(2×4) were made in another ultrahigh vacuum (UHV) system using the Omicron instrument. The filled-state imaging was performed in the constant current mode with a tunneling current of 0.1–0.3 nA and a bias voltage of 2–4 V. All the photoemission and STM measurements were done at room temperature.

The InAs samples were grown by MBE on epiready *n*-type GaSb(100) and InAs(100) substrates. The GaSb substrates were annealed in the MBE chamber under vacuum to 350 °C and in Sb flux up to 500 °C. After the native oxide desorption, a thin GaSb buffer layer was deposited on GaSb(100) at the substrate temperature of 450 °C. Growth of the few hundreds of angstroms thick GaSb epilayer gave a smooth surface, as assessed by reflection high-energy electron diffraction (RHEED), with two-dimensional streaky RHEED patterns. Directly after the GaSb buffer deposition the InAs epilayer was grown in the 2×4 conditions, monitored by RHEED, at 450 °C with a growth rate of 0.1 ML/s. The InAs buffer layer was grown in the same conditions on InAs(100). RHEED showed a sharp 2×4 pattern for all the substrates upon the growth of the InAs film, and the pattern remained fairly during the sample cooling. These InAs(100)(2×4) samples were quickly transferred under UHV to the analysis chamber of the 41 beamline. The as-grown (2×4) surfaces were heated for ≈10 min in the UHV conditions at different temperatures in the range of 300–400 °C. Low-energy-electron-diffraction (LEED) observations were done for the as-grown InAs(100)(2×4) surface and after each heating step of the same sample, before the photoemission measurements. LEED showed a clear 2×4 pattern with low background for the as-grown surface. The 2×4 pattern became somewhat sharper after the heating at 300 °C most likely due to the desorbing of some excess of As, adsorbed on the (2×4) surface in MBE during the sample cooling and transfer, agreeing with the core-level results below. The sharp 2×4 pattern remained after annealing at 300–350 °C, and quality of the LEED patterns showed the ordered InAs(100)(2×4) surfaces. The heating higher than 360 °C weakened the pattern and changed it into a mixture of the 2×4 and 4×2 symmetries. Above 390 °C, only a clear 4×2 pattern was observed. These LEED observations agree well with previous studies.[7]

The Sb-induced InAs(100)(2×4) reconstruction was prepared by MBE: The InAs(100)(2×4) sample was heated in vacuum to 350 °C and then up to 500 °C in Sb_4 flux monitoring RHEED simultaneously. When the Sb flux was opened, the pattern changed quickly to a 1×3 one. As the temperature was increased under the Sb flux, a 2×4 pattern loomed up and became sharp near 500 °C. After the cooling and Sb-flux termination the sample was transferred back to the analysis chamber. The sample was heated at 300–350 °C

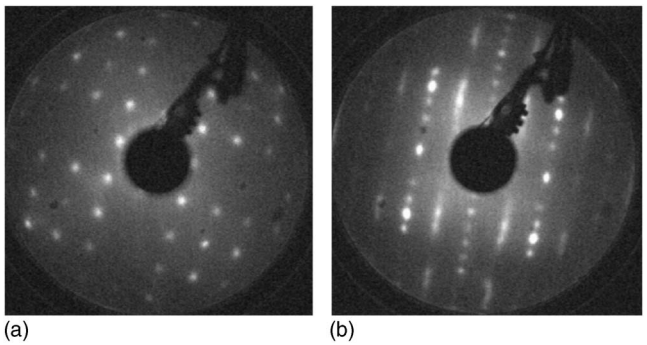

FIG. 2. LEED patterns from the As-decapped GaAs(100) surface: (a) $c(4\times4)$ at 47 eV after the heating at 330 °C, (b) 2×4 at 113 eV after the heating at 500 °C.

in UHV, to keep the (2×4) reconstruction judged by LEED before photoemission measurements.

For investigating the GaAs(100)(2×4) by photoemission, we prepared the GaAs(100)$c(4\times4)$ surface by MBE with *in situ* RHEED after the GaAs buffer growth. The sample was transferred into the analysis chamber under vacuum conditions and heated there in UHV to obtain a clear 2×4 LEED pattern.

Another GaAs substrate was used for STM. The As-capping layer was deposited after the growth of about 300 -nm buffer layer on the GaAs(100). After the transfer through air, the cap layer was removed by heating the sample in UHV at 330 °C for ≈12 h. This produced the $c(4\times4)$ reconstruction as deduced by STM and LEED [Fig. 2(a)]. The $c(4\times4)$ surface was heated, as the photoemission sample, and LEED and STM measurements were performed after each heating step. Within these two UHV systems, we obtained the 2×4 LEED pattern from the GaAs surface [Fig. 2(b)] in the temperature range of 410–520 °C. The temperature was measured in the both vacuum systems by an infrared thermometer with an estimated error of ±30 °C. After 550 °C the 2×4 pattern disappeared, and the 4×2 combined with $n\times6$ one loomed up and became sharper at 600 °C. These LEED observations are consistent with previous experiments (Ref. 10, and references therein).

III. RESULTS AND DISCUSSION

A. Scanning tunneling microscopy for GaAs(100)(2×4)

A filled-state STM image of the GaAs(100) surface, which exhibited the 2×4 LEED pattern upon the heating at 500 °C, is shown in Fig. 3(a). The image is characterized by rows running in the [0–11] direction. A separation of the rows in the [011] direction (i.e., perpendicular to the rows' direction) is ≈16 Å indicating the $\times4$ periodicity. The brighter areas in Fig. 3(a) are due to terraces. Kinks are also observed in the rows. The ordered domains between (point-like) defects or kinks are typically 5–15 nm in diameter; i.e., somewhat smaller than what has been observed earlier for an MBE-grown GaAs(100)(2×4) surface,[6] as can be readily expected from the difference in the preparation conditions. A high-resolution filled-state image from an ordered domain of the same surface is presented in Fig. 3(b). The rows consist of bright protrusions slightly oval in shape along the rows (i.e., in the [0–11] direction). One of those protrusions is marked by the arrow *A* in the image. The distance between the protrusions in the [0-11] direction is ≈8 Å corresponding to the $2\times$ periodicity. The darker protrusions, labeled *B*, also arrange the $2\times$ periodicity, but the $2\times$ rows arranged by the *A* and *B* protrusions are out of the phase. This shift in the [0–11] direction is very similar to that found in Ref. 11. We also attribute the protrusion *B* to the third-layer As dimer because imaging the filled density of states, one probes dangling bonds of the As atoms.[36] The appearance of the third-layer As dimers is consistent with both the $\beta2$ and $\alpha2$ models. However, the $\beta2$ structure is excluded here because (i) the *A* protrusions are clearly more slender in the [011] direction (i.e., perpendicular to the rows) than the corresponding ones of the $\beta2$ phase in Refs. 5, 6, and 11 and (ii) the *B* rows locate asymmetrically between the *A* rows, which is not the case for the two-top-dimer $\beta2$ surface.[11] Hence, we relate the protrusion *A* to just one As dimer in the top layer. The appearance of gray features between the protrusions *A* and *B* also agrees with the $\alpha2$ geometry, where the second-layer Ga dimers can show up.[14] Indeed, our STM observations give support to the existence of the GaAs(100)$(2\times4)\alpha2$ domains. To establish this surface structure, substantiating evidence is needed.

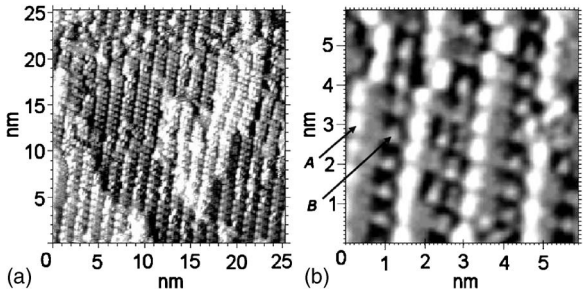

FIG. 3. (a) A filled-state STM image from the GaAs(100) surface which showed the 2×4 LEED pattern after heating at 500 °C. The image is characterized by rows running in the [0-11] direction: the tunneling current is 0.28 nA and bias voltage 2.0 V. (b) A high-resolution filled-state image of the (2×4) domain on the same surface: the tunneling current is 0.22 nA and bias voltage 1.9 V.

B. Core-level photoemission from Sb-induced InAs(100)(2×4)

It is important to determine justifiably the core-level-line shape for the components used in the deconvolution. To this end concerning the As 3*d* spectra, we studied the As 3*d* emission from an Sb-induced InAs(100)(2×4) surface (Fig. 4). This As 3*d* spectrum can be fitted well by one component, i.e., spin-orbit doublet labeled *B*, using the standard methods with the Voigt-profile peaks. The background was subtracted by the Shirley's method as for all the spectra of the InAs system. The fitting parameters for *B* in Table I are consistent with those used previously.[21–28,35] It is our claim that the component *B* originates from the InAs bulk. Anyhow, the *B* gives an upper limit on the linewidth of As 3*d*, and this line shape (i.e., the Voigt peaks with the same parameters as for

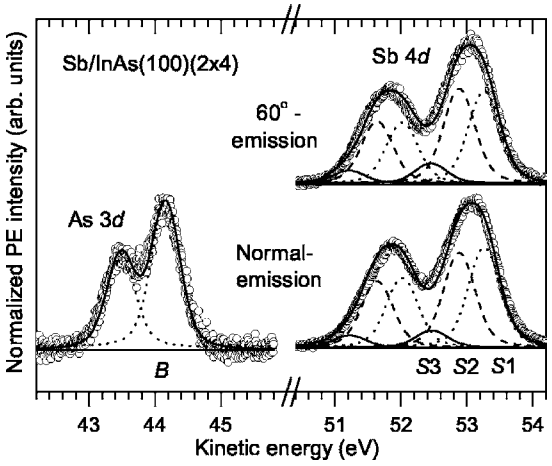

FIG. 4. The As 3*d* spectrum from the Sb/InAs(100)(2×4) surface heated at 300 °C and the Sb 4*d* spectra heated at 350 °C. The spin-orbit-doublet components and results of the fits (the solid lines through the data points) are also shown. The photon energy is 90 eV. The fitting parameters are in Table I.

B) has been used for all the As 3*d* components of InAs(100)(2×4) below. The Gaussian width has been allowed to vary slightly between the different spectra (Table I), which is assumed to reflect differences in the bonding homogeneity at the surface layer(s) and/or phonon broadening.[21,25,37–39] The remaining parameters, namely, a number of the components and their energy positions and relative intensities were obtained as a result of the deconvolution process. We remark that in this work the energy positions and shifts of the components were not fixed between the different surfaces, but the same SCLS's were required for the individual surface with the different emission angles and photon energies.

Deconvolution of the Sb 4*d* spectra for the Sb/InAs(100)(2×4) surface, shown in Fig. 4, reveals two dominating components *S*1 and *S*2 with the splitting of 0.38 eV. The third signal *S*3 is distinctly weaker, about 10% of the total intensity, which indicates that *S*3 originates from local defects. With only one dominating component (*S*1- or *S*2-like one) in addition to the *S*3, the Gaussian width would be 0.74 eV. We find no clear reason for such wide Sb components on a clean long-range-ordered Sb/InAs(100)(2×4) surface. Therefore, we conclude the presence of both *S*1 and *S*2 in these Sb spectra. The *S*3 is needed to obtain an acceptable fitting.

Proposing origins of these components, we consider first whether the Sb atoms deeper, in the bulklike environment, could cause the component(s) since previous investigations have shown reconstruction-enhanced solubility of group-V elements in III-V's.[40] This is, however, unlikely because the Sb spectra with different surface sensitivities are similar to each other, and none of the Sb components has a relative bulk sensitivity. We also believe that using Sb_4 in our experiment hinders the bulk diffusion more efficiently than would Sb_2 do.[41,42] Thus, *S*1, *S*2, and *S*3 are proposed to arise from surface layer(s).

TABLE I. Fitting parameters for the As 3*d*, In 4*d*, and Sb 4*d* core-level spectra of the InAs(100)(2×4) and Sb/InAs(100)(2×4) surfaces. All energies are in eV.

	As 3*d*	In 4*d*	Sb 4*d*
Spin-orbit splitting	0.68	0.855	1.243
Branching ratio	0.64±0.02	0.67±0.02	0.68±0.02
Lorentzian width	0.16	0.16	0.16
Gaussian width	0.43±0.02	0.40±0.02	0.48

We assign *S*3 to a local pure Sb—Sb bonding. This is reasonable because excess Sb can be adsorbed on the Sb/InAs(100)(2×4) during sample cooling. The Sb layer is known to be more stable than the As surface layer,[43] and may withstand annealing at 350 °C. The components *S*1 and *S*2, as we understand them, are due to the emission from two different bonding sites of Sb in the (2×4) structure, in accordance with earlier observations on similar Sb/GaAs(100)(2×4) surfaces.[35]

To the best of our knowledge, there exists only one structural model proposed for the Sb/InAs(100)(2×4) surface.[44] Grosse *et al.*[44] have reported the STM finding of an $\alpha 2$ phase on Sb/InAs(100)(2×4) with two nonequivalent Sb-dimer sites per unit cell with the 1:1 occupation proportion. This finding supports our Sb 4*d* interpretation that the *S*1 and *S*2, with nearly identical intensities, originate from the nonequivalent Sb-dimer sites in Sb/InAs(100)(2×4).

C. Core-level photoemission from InAs(100)(2×4)

Figure 5 shows the As spectra measured in different surface-sensitive conditions from the InAs(100)(2×4) surfaces heated up to 330 °C. The deconvolution exhibits two SCLS's, *S*1 and *S*2, and the InAs bulk one *B* for all the (2×4) surfaces, indicating that arsenic has two different bonding environments in the reconstruction. Moreover, the third SCLS, *S*3, was required to reproduce the line shape of the as-grown (2×4) surface. *S*3 is shifted by 0.60 eV to the lower kinetic energy from *B*. Energetically, it resembles the emission found previously on an As-super-rich GaAs(100) surface.[45] Thus, *S*3 can be related to extra As atoms on the surface bonding only to As (i.e., As—As), which agrees well with the experimental conditions of this work, as noticed in Sec. II. The surface sensitivity of *S*3 also supports this assignment. From the relative *S*3 intensity, we estimate such an As-defect density to be ≈15% on the as-grown (2×4) surfaces, which is somewhat higher than that (≈5%) observed recently on InAs(100)(2×4) by STM.[46] According to the core-level results, the heating at 300 °C or lower removes these defects from the InAs surface, in consistency with that extra As desorbs easily from the III-V surfaces at this temperature.[43]

There are no clear structures in the As spectra of Fig. 5. As noticed in Sec. I, to justify the existence of the *S*1 and *S*2 in As 3*d* of the InAs(100)(2×4), we construct and analyze a difference line shape $D(E)$ for the two As spectra which have been measured with the different surface sensitivities from the surface after heating at 300 °C. Following the procedure in Ref. 47, we subtracted a weighted bulk sensitive spectrum $I_B(E)$ (the middle spectrum in the left panel of Fig. 5) from

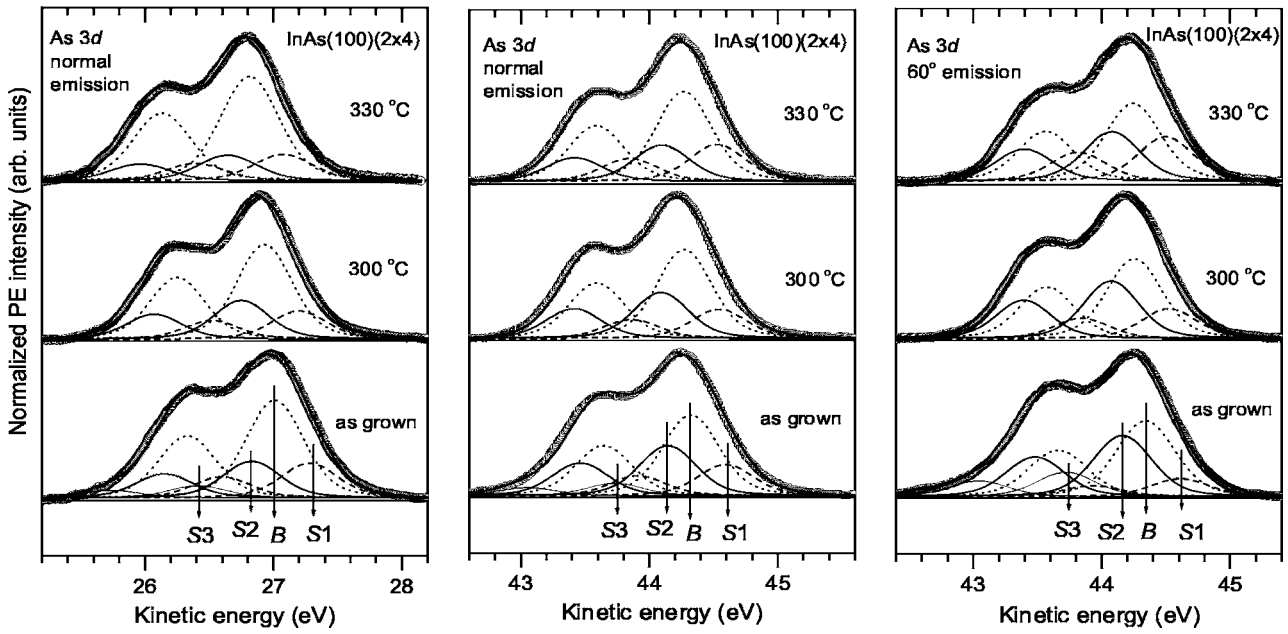

FIG. 5. The As 3*d* spectra measured in different surface-sensitivity conditions, spin-orbit-doublet components, and results of the fits (the solid lines through the data points) for the InAs(100)(2×4) surfaces heated at different temperatures. The photon energy is about 72 eV in the left panel and 90 eV in the middle and right panels. The fitting parameters and results are listed in Tables I and II. The arrows show the $d_{5/2}$ positions of the components approximately.

the more surface sensitive spectrum $I_S(E)$ (the right panel one) to obtain an approximation to the surface-core-level-line shape, in which the bulk contribution is neglected. That is,

$$D(E) = I_S(E) - \lambda I_B(E), \tag{1}$$

where $0 \leqslant \lambda \leqslant 1$ is a weight factor and E is the energy. The positions of the bulk $d_{5/2}$ peaks of As and In have been used to align the spectra. Indeed, these $D(E)$ line shapes in Fig. 6 reveal at least two SCLS's. One of them is shifted about 0.2 eV to the lower kinetic energy, and the other locates at 0.2–0.3 eV in the high-kinetic-energy side. Based on the relative component intensities (Table II), one can estimate that the $D(E)$ at the weight of 0.8 exhibits the surface-core-level line shape of As 3*d* in which the bulk contribution is neglected. The aforementioned *S*1 and *S*2 produce the reasonable fitting of this approximate surface spectrum (the bottom of Fig. 6). Moreover, a similar $D(E)$ spectrum is shown in Fig. 7, where the As 3*d* emission for the Sb/InAs(100)×(2×4) surface in Fig. 4, weighted with λ, is subtracted from the As 3*d* of the InAs(100)(2×4) surface heated at 300 °C. From the fitting results, the $D(E)$ at the weight of 0.5 represents an approximation to the surface-core-level line shape of the InAs(100)(2×4). All these results in Figs. 4–7 together verify the presence of the *S*1 and *S*2 in As 3*d* of the InAs(100)(2×4) surface.

The absence of *S*1 and *S*2 in As 3*d* of the Sb/InAs(100)×(2×4) surface proposes that As atoms, which cause *S*1 and *S*2 in As 3*d* of the InAs(100)(2×4) surface, disappear in the structure of Sb/InAs(100)(2×4). This is well consistent with the idea that As-dimer atoms desorb, and are subsequently substituted by Sb, as occurs on Sb/GaAs(100)(2×4).[28] To elucidate atomic origins of the As-derived *S*1 and *S*2 of the InAs(100)(2×4) surfaces, we study the intensity ratio *S*2/*S*1. On the basis of previous investigations,[7,12,13,15,16] the β2 phase or the α2 phase or a combination of these two domains exists on the InAs(100)×(2×4). The both β2 and α2 consist of two inequivalent

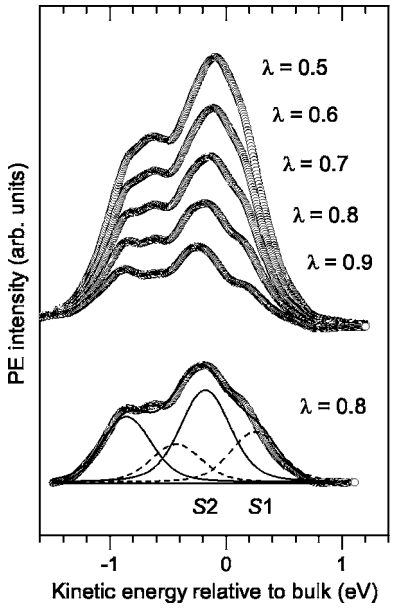

FIG. 6. The top: the difference line shapes between two As 3*d* spectra of Fig. 5 measured in the surface- (right panel) and bulk-sensitive conditions (left panel) after heating at 300 °C at the weights (λ) of 0.5–0.9. The bottom: deconvolution of the 0.8-weight line shape in which the bulk component is estimated to be neglected (see text).

TABLE II. The As 3*d* results from the InAs(100)(2×4) surfaces heated at different temperatures. Energy shifts of the As surface components *S*1 and *S*2 are referenced to the bulk component *B*. The − sign indicates a shift toward the lower kinetic energy. All energies are in eV. The relative intensities of the surface components have been determined from the spectra with the less, (more), and [most] surface sensitive conditions in the left, (middle), and [right] panels of Fig. 5, respectively.

	*S*1 shift	*S*2 shift	*S*1/*B*	*S*2/*B*	*S*2/*S*1
as grown	0.27	−0.18	0.33 (0.38) [0.24]	0.45 (0.62) [0.80]	1.36 (1.63) [3.33]
300 °C	0.27	−0.18	0.30 (0.33) [0.38]	0.41 (0.52) [0.73]	1.37 (1.58) [1.92]
330 °C	0.26	−0.17	0.25 (0.41) [0.57]	0.24 (0.40) [0.63]	0.96 (0.98) [1.11]

As-dimer sites per unit cell, i.e., the first-layer and third-layer dimers (Fig. 1). For the $\beta 2$ phase, the occupation proportion of the first-layer sites to the third-layer sites is 2:1, whereas for the $\alpha 2$ phase it is 1:1. The ratio *S*2/*S*1 is close to unity for the InAs(100)(2×4) surface heated at 330 °C (Table II), lending support to the presence of the $\alpha 2$ phase in good agreement with previous STM results.[7] The ratio *S*2/*S*1 is larger for the as-grown surface and that heated at 300 °C, indicating the appearance of the $\beta 2$ domains on those surfaces. Although all the photoelectron attenuation and diffraction effects have been ignored here, the *S*2/*S*1 ratios determined from the various spectra (Table II) and the difference line shapes (Figs. 6 and 7) clearly show that the intensity of *S*2 is higher than the *S*1 intensity on the as-grown surface and after the heating at 300 °C. Therefore, *S*1 can be related to the third-layer As-dimer site and *S*2 to the top-layer site at the InAs(100)(2×4) surfaces studied. The assignment is supported by the observation that the *S*2 intensity decreased when the temperature was increased. This indicates a partial reevaporation of the first layer As atoms from the InAs(100)(2×4) surface at 330 °C, in good agreement with previous studies which have shown that the transition to the $\alpha 2$ phase involves desorption of the first-layer dimers from the $\beta 2$ surface.[7,16]

The In 4*d* spectra from the as-grown InAs(100)(2×4) surface and that heated at 300 °C are found to involve two SCLS's (Fig. 8). Here, *S*1 is shifted by 0.23 eV towards the higher kinetic energy from *B* and *S*2 to the lower kinetic energy by 0.30 eV. The corresponding shifts of the surface heated at 330 °C are 0.21 and 0.29 eV. The In 4*d* spectra and fittings for the Sb/InAs(100)(2×4) reconstruction (not shown) are very similar to those in Fig. 8 with the same shifts. The presence of two In-related SCLS's agrees with the behavior of Ga on the GaAs(100)(2×4) and Sb/GaAs(100)(2×4) surfaces previously.[25,35] Thus, we propose that *S*1 and *S*2 arise from the second-layer In atoms (note that the environment of the fourth-layer In resembles the fourfold-coordinated bulk). According to the $\beta 2$ model, indium has two inequivalent sites in the second layer: (i) a threefold-coordinated site bonded to the As dimer and (ii) a fourfold-coordinated site, between two threefold-coordinated ones, bonded to two As dimers. The number of the threefold-coordinated In atoms is twice of the number of fourfold-coordinated atoms. We are inclined to suggest that *S*1, of

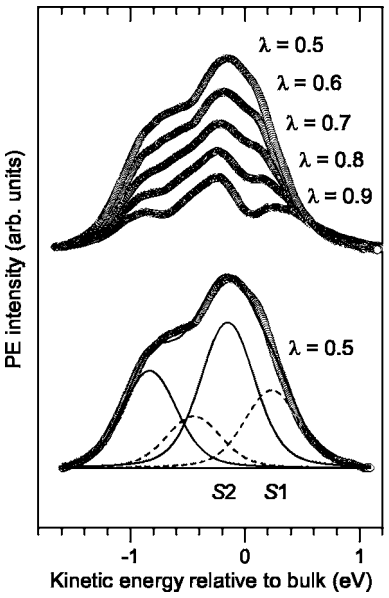

FIG. 7. Similar difference line shapes to Fig. 6 but between the As spectrum of InAs(100)(2×4) in the right panel after 300 °C and the As spectrum of the Sb/InAs(100)(2×4) surface in Fig. 4, and the deconvolution of the 0.5-weight line shape in which the bulk component is estimated to be neglected.

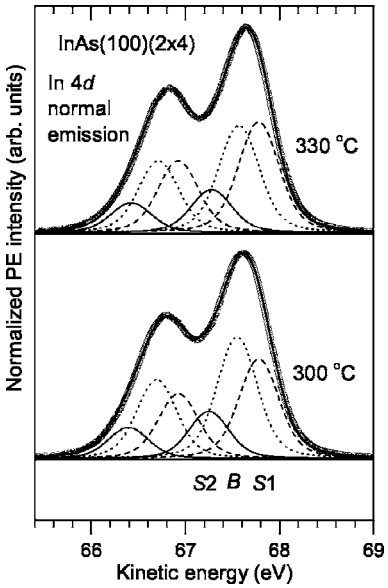

FIG. 8. The In 4*d* spectra of the InAs(100)(2×4) surfaces. The photon energy is 90 eV. The component shifts are described in the text.

TABLE III. The As 3*d* results from the GaAs(100)(2×4) surfaces heated at different temperatures. Energy shifts of the As surface components *S*1 and *S*2 are referenced to the bulk component *B*. The − sign indicates a shift toward the lower kinetic energy. All energies are in eV. The relative intensities of the surface components have been determined from the spectra with the bulk- and (surface)-sensitive conditions in the left and (right) panels of Fig. 9, respectively.

	*S*1 shift	*S*2 shift	*S*1/*B*	*S*2/*B*	*S*2/*S*1
390 °C	0.31	−0.17	0.32 (0.43)	0.40 (0.65)	1.25 (1.51)
420 °C	0.30	−0.17	0.35 (0.39)	0.40 (0.70)	1.14 (1.79)
465 °C	0.29	−0.16	0.35 (0.50)	0.35 (0.51)	1.00 (1.02)

which intensity is higher than *S*2, arises from the threefold-coordinated In site and *S*2 from the fourfold-coordinated site on the surface heated at 300 °C. However, this identification is uncertain since the $\alpha 2$ phase may be present and that phase includes three inequivalent second-layer In sites (Fig. 1). On the surface heated at 330 °C, where the $\alpha 2$ phase can be clearly expected to dominate, *S*1 and *S*2 appear at about the same energies as those in the lower-temperature samples, which have the $\beta 2$ domains. The results here do not allow us to discuss possible origins of *S*1 and *S*2 among the second-layer In sites of the $\alpha 2$ model. Thus, we only note that the energy shifts and relative intensities of *S*1 and *S*2 of the $\alpha 2$ surface are consistent with those found below for Ga 3*d* of the GaAs(100)(2×4) surface.

D. Core-level photoemission from GaAs(100)(2×4)

We have utilized the previous As 3*d* line shape measured from the Sb/GaAs(100)(2×4) surface under the same experimental conditions,[35] to get a similar maximum-linewidth approach for fitting the As spectra of the GaAs(100)×(2×4). These fitting parameters, except the Gaussian width of 0.48±0.02 eV, are identical to those in Table I for the InAs system. The slightly higher Gaussian width for the GaAs(100)(2×4) than for InAs(100)(2×4) can be due to the surface inhomogeneities and/or phonon broadening.[21,25,37–39] We note that the linear background was subtracted from the As spectra measured at the photon energy of 65 eV, whereas the Shirley's method was used for the other spectra. The results are compiled in Table III.

The As 3*d* spectra and deconvolutions are shown in Fig. 9. Two SCLS's (*S*1 and *S*2) and the GaAs bulk one *B* appear on the (2×4) surfaces heated at different temperatures. *S*3 is resolved for the surface heated at 390 °C. It is very similar to that found on the InAs(100)(2×4) surface. Thus, *S*3 is connected to defects related to the extra As on the GaAs(100)(2×4), which is reasonable with our experiments and the fact that the GaAs surfaces can be heated at higher temperatures than the InAs surfaces keeping still the As-stabilized structure.[6,7,15,16] According to previous investigations,[4–6,8–11] the $\beta 2$ phase can be expected on the present GaAs(100)(2×4) surface heated at 420 °C. In fact, the preparation parameters for that surface are almost identical with those of the $\beta 2$ phase in Ref. 6. Based on the intensity ratio, we attribute *S*1 to the third-layer dimers and *S*2 to the top-layer dimers. These two shifts are very similar to the *S*1 and *S*2 of InAs(100)(2×4), and their intensity ratios behave similarly with the increasing temperature. Furthermore, the difference line shapes (Fig. 10), which have been obtained by subtracting the left panel spectrum at 420 °C $[I_B(E)]$, weighted with λ, from the right panel one $[I_S(E)]$, justify the existence of the *S*1 and *S*2. Sustaining the above STM observations, the As 3*d* results propose the GaAs(100)(2×4)$\alpha 2$ domains to appear after the UHV heating of the $\beta 2$ surface.

Let us still compare the As components *S*1 and *S*2 identified for the InAs(100)(2×4) and GaAs(100)(2×4) in this work with those reported in the literature.[21,22,25–27] The energy separation between our *S*1 and *S*2 (0.4–0.5 eV) is clearly smaller than about 0.8 eV reported earlier for the GaAs(100)(2×4) reconstruction.[21,22,25–27] The present *S*1 shift relative to *B* agrees reasonably with the published val-

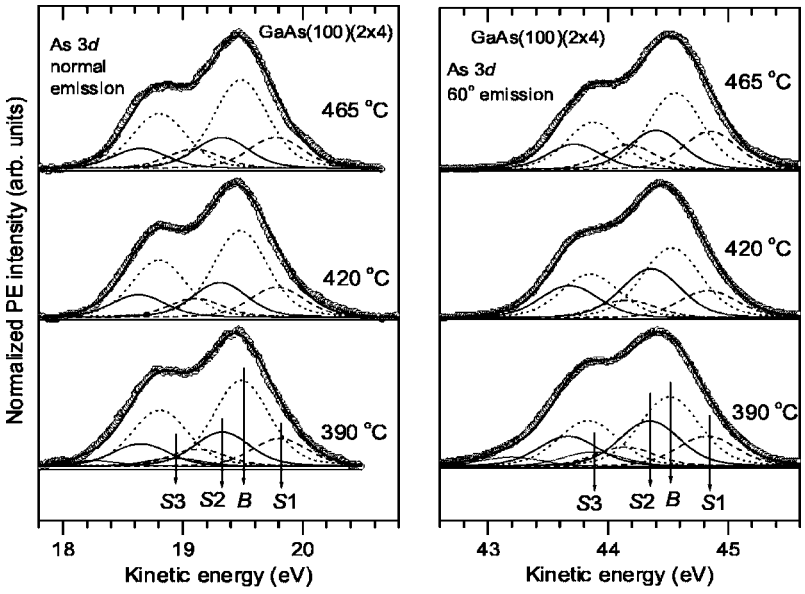

FIG. 9. The As 3*d* spectra measured in different surface-sensitivity conditions, spin-orbit-doublet components, and results of the fits (solid lines through data points) for the GaAs(100)(2×4) surfaces heated at different temperatures. The photon energy is 65 eV in the left panel and 90 eV in the right panel. The fitting results are listed in Table III. The arrows show the $d_{5/2}$ positions of the components approximately.

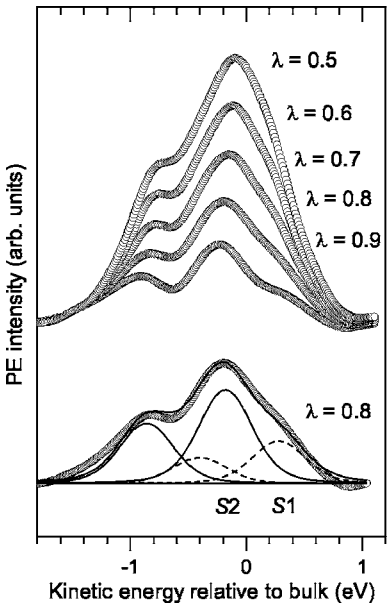

FIG. 10. Similar difference spectra to Fig. 6 but for GaAs(100)(2×4) between two As 3*d* spectra of Fig. 9 after heating at 420 °C, and the deconvolution of the 0.8-weight spectrum in which the bulk component is estimated to be neglected.

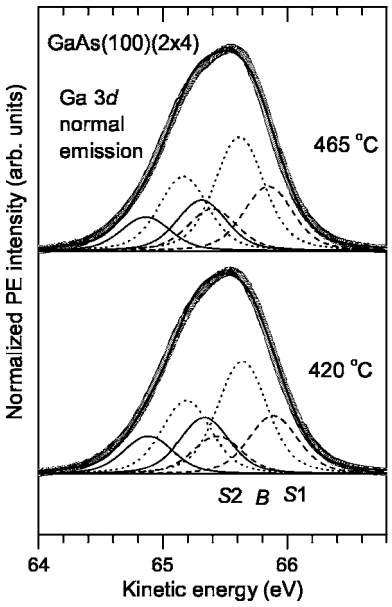

FIG. 11. The Ga 3*d* spectra and deconvolutions for the GaAs(100)(2×4) surfaces. The photon energy is 90 eV. The component properties are in the text.

ues, but the *S*2 does not, indicating that the *S*2 is not the same component as previous ones. We note that the energy separation between *S*1 and *S*2 is consistent with that of two Sb 4*d* components observed on Sb/InAs(100)(2×4) and earlier on the Sb/GaAs(100)(2×4)α2 surface.[35] Theoretical calculations are needed to solve physical phenomena beyond these SCLSs. Unfortunately, no such SCLS calculations are available for the III–V(100)(2×4) surfaces, to our knowledge. Tentatively, we speculate that due to the higher spatial position of the first-layer dimers, the core-hole screening in photoemission might be reduced for them, as compared to third-layer dimers, resulting in a lower kinetic energy of photoelectron from the first-layer site.

Finally, the Ga 3*d* spectra of the GaAs(100)(2×4) surfaces in Fig. 11 are considered. The fitting parameters are the same as in Ref. 35: spin-orbit splitting=0.45 eV, branching ratio=0.66±0.01, Lorentzian width=0.16 eV, and Gaussian width=0.39±0.02 eV. Two SCLS's are resolved in the Ga spectra: *S*1 is shifted by 0.25 eV (0.23 eV) to the higher kinetic energy from *B* and *S*2 to the lower kinetic energy by 0.31 eV (0.30 eV) on the surface heated at 420 °C (465 °C). These shifts and the *S*2/*S*1 intensity ratios agree quite well with those of two In 4*d* SCLS's discussed above.

IV. CONCLUSIONS

The As 3*d* core-level studies, including the analysis of the difference spectra and emission from the Sb-induced (2×4) surface, demonstrate that the As 3*d* emission from technologically important III-As(100)(2×4) surfaces consists of two SCLS's which are shifted about 0.3 eV (*S*1) and 0.2 eV (*S*2) to the higher and lower kinetic energy from the bulk, respectively. On the basis of the *S*2/*S*1 intensity ratios, the *S*1 is connected to the third-layer As-dimer site and the previously unobserved *S*2 to the top-layer As-dimer site in the established structural model. The STM observation of the GaAs(100)(2×4)α2 structure, combined with the comparison of the core-level results between GaAs(100)(2×4) and InAs(100)(2×4), gives experimental support to the appearing of the α2 domains on the GaAs(100)(2×4) surface, as predicted in the theory.

ACKNOWLEDGMENTS

The authors wish to thank Professor Q.-K. Xue for valuable discussions and Mr. H. Ollila for technical assistance. We are grateful for the assistance received from the MAX-lab staff. One of us (P.L.) would like to acknowledge financial support by *Graduate School of Materials Research* (Finland), and four of us would like to acknowledge financial support by the EC *Access to Research Infrastructure Program*. J. S. acknowledges the financial support from the Polish State Committee for Scientific Research (KBN) through Grants Nos. 2-P03B-05423 and PBZ-KBN-044/P03/2001. This work has been supported in part by the Academy of Finland Grant No. 205766 (I.J.V.).

*Email address: pekka.laukkanen@utu.fi
†Also at A. F. Ioffe Physico-Technical Institute, Russian Academy of Sciences, St. Petersburg 194021, Russian Federation.

[1] J. R. Arthur and J. J. LePore, J. Vac. Sci. Technol. **6**, 545 (1969).
[2] A. Y. Cho, J. Appl. Phys. **42**, 2074 (1971).
[3] W. G. Schmidt, P. H. Hahn, F. Bechstedt, N. Esser, P. Vogt, A. Wange, and W. Richter, Phys. Rev. Lett. **90**, 126101 (2003).
[4] J. E. Northrup and S. Froyen, Phys. Rev. B **50**, 2015 (1994).
[5] T. Hashizume, Q.-K. Xue, J. Zhou, A. Ichimiya, and T. Sakurai, Phys. Rev. Lett. **73**, 2208 (1995).
[6] T. Hashizume, Q.-K. Xue, A. Ichimiya, and T. Sakurai, Phys. Rev. B **51**, 4200 (1995).
[7] H. Yamaguchi and Y. Horikoshi, Phys. Rev. B **51**, 9836 (1995).
[8] W. G. Schmidt and F. Bechstedt, Phys. Rev. B **54**, 16742 (1996).
[9] Y. Garreau, M. Sauvage-Simkin, N. Jedrecy, R. Pinchaux, and M. B. Veron, Phys. Rev. B **54**, 17 638 (1996).
[10] Q.-K. Xue, T. Hashizume, and T. Sakurai, Prog. Surf. Sci. **56**, 1 (1997).
[11] V. P. LaBella, H. Yang, D. W. Bullock, P. M. Thibado, P. Kratzer, and M. Scheffler, Phys. Rev. Lett. **83**, 2989 (1999).
[12] M. Göthelid, Y. Garreau, M. Sauvage-Simkin, R. Pinchaux, A. Cricenti, and G. Le Lay, Phys. Rev. B **59**, 15 285 (1999).
[13] C. Ratsch, W. Barvosa-Carter, F. Grosse, J. H. G. Owen, and J. J. Zinck, Phys. Rev. B **62**, R7719 (2000).
[14] W. G. Schmidt, S. Mirbt, and F. Bechstedt, Phys. Rev. B **62**, 8087 (2000).
[15] R. H. Miwa and G. P. Srivastava, Phys. Rev. B **62**, 15 778 (2000).
[16] F. Grosse, W. Barvosa-Carter, J. J. Zinck, and M. F. Gyure, Phys. Rev. B **66**, 75321 (2002).
[17] L. D. Broekman, R. C. G. Leckey, J. D. Riley, A. Stampfl, B. F. Usher, and B. A. Sexton, Phys. Rev. B **51**, 17 795 (1995).
[18] D. E. Eastman, T.-C. Chiang, P. Heimann, and F. J. Himpsel, Phys. Rev. Lett. **45**, 656 (1980).
[19] E. Pehlke and M. Scheffler, Phys. Rev. Lett. **71**, 2338 (1993).
[20] J. C. Woicik, P. Pianetta, and T. Kendelewicz, Phys. Rev. B **40**, 12 463 (1989).
[21] C. J. Spindt, M. Yamada, P. L. Meissner, K. E. Miyano, T. Kendelewicz, A. Herrera-Gomez, W. E. Spicer, and A. J. Arko, Phys. Rev. B **45**, 11 108 (1992).
[22] R. Ludeke, T.-C. Chiang, and D. E. Eastman, Physica B & C **117** & **118,** 819 (1983).
[23] J. F. van der Veen, P. K. Larsen, J. H. Neave, and B. A. Joyce, Solid State Commun. **49**, 659 (1984).
[24] A. D. Katnani, H. W. Sang, Jr., P. Chiaradia, and R. S. Bauer, J. Vac. Sci. Technol. B **3**, 608 (1985).
[25] G. Le Lay, D. Mao, A. Kahn, Y. Hwu, and G. Margaritondo, Phys. Rev. B **43**, 14301 (1991).
[26] I. M. Vitomirov, A. Raisanen, A. C. Finnefrock, R. E. Viturro, L. J. Brillson, P. D. Kirchner, G. D. Pettit, and J. M. Woodall, Phys. Rev. B **46**, 13293 (1992).
[27] P. Moriarty, B. Murphy, L. Roberts, A. A. Cafolla, G. Hughes, L. Koenders, and P. Bailey, Phys. Rev. B **50**, 14 237 (1994).
[28] F. Maeda, Y. Watanabe, and M. Oshima, Phys. Rev. B **48**, R14 733 (1993).
[29] M. Sugiyama, S. Maeyama, F. Maeda, and M. Oshima, Phys. Rev. B **52**, 2678 (1995).
[30] P. Moriarty, P. H. Beton, Y.-R. Ma, M. Henini, and D. A. Woolf, Phys. Rev. B **53**, R16 148 (1996).
[31] N. Esser, A. I. Shkrebtii, U. Resch-Esser, C. Springer, W. Richter, W. G. Schmidt, F. Bechstedt, and R. Del Sole, Phys. Rev. Lett. **77**, 4402 (1996).
[32] T.-L. Lee and M. J. Bedzyk, Phys. Rev. B **57**, R15 056 (1998).
[33] F. Maeda and Y. Watanabe, Phys. Rev. B **60**, 10 652 (1999).
[34] L. J. Whitman, B. R. Bennett, E. M. Kneedler, B. T. Jonker, and B. V. Shanabrook, Surf. Sci. **436**, L707 (1999).
[35] P. Laukkanen, R. E. Perälä, R.-L. Vaara, I. J. Väyrynen, M. Kuzmin, and J. Sadowski, Phys. Rev. B **69**, 205323 (2004).
[36] M. D. Pashley, Phys. Rev. B **40**, 10 481 (1989), and references therein.
[37] T. Kendelewicz, P. H. Mahowald, K. A. Bertness, C. E. McCants, I. Lindau, and W. E. Spicer, Phys. Rev. B **36**, 6543 (1987).
[38] G. Le Lay, J. Kanski, P. O. Nilsson, U. O. Karlsson, and K. Hricovini, Phys. Rev. B **45**, 6692 (1992).
[39] J. M. C. Thornton, P. Weightman, D. A. Woolf, and C. J. Dunscombe, J. Electron Spectrosc. Relat. Phenom. **72**, 65 (1995).
[40] S. B. Zhang and A. Zunger, Appl. Phys. Lett. **71**, 677 (1997).
[41] M. W. Wang, D. A. Collins, T. C. McGill, and R. W. Grant, J. Vac. Sci. Technol. B **11**, 1418 (1993).
[42] D. A. Collins, M. W. Wang, R. W. Grant, and T. C. McGill, J. Vac. Sci. Technol. B **12**, 1125 (1994).
[43] J. J. Zinck, E. J. Tarsa, B. Brar, and J. S. Speck, J. Appl. Phys. **82**, 6067 (1997).
[44] F. Grosse, W. Barvosa-Carter, J. J. Zinck, and M. F. Gyure, J. Vac. Sci. Technol. B **20**, 1178 (2002).
[45] P. K. Larsen, J. H. Neave, J. F. van der Veen, P. J. Dobson, and B. A. Joyce, Phys. Rev. B **27**, 4966 (1983).
[46] W. Barvosa-Carter, R. S. Ross, C. Ratsch, F. Grosse, J. H. G. Owen, and J. J. Zinck, Surf. Sci. **499**, L129 (2002).
[47] A. Goldoni, S. Modesti, V. R. Dhanak, M. Sancrotti, and A. Santoni, Phys. Rev. B **54**, 11 340 (1996).